Int J Adv Manuf Technol (2013) 69:627–636
DOI 10.1007/s00170-013-5042-6

ORIGINAL ARTICLE

An analytical model for the collapsing deformation of thin-walled rectangular tube in rotary draw bending

K. X. Liu · Y. L. Liu · H. Yang

Received: 27 December 2012 / Accepted: 29 April 2013 / Published online: 22 May 2013

Abstract The collapsing deformation of an outer flange is the key factor affecting the forming quality of a thin-walled rectangular tube during the rotary draw bending process. Therefore, the collapsing deformation is a problem that needs an urgent solution. Firstly, based on the simplified model for loads and deformation of the outer flange, the force acted by the core die and the bending moment acted by the clamp die are obtained analytically. Then, the analytical formula of collapsing deformation is deduced based on the theory of plate and shell, and finally, the analytical model is validated by comparison with simulated and experimental results. The study is of great significance to elevate the forming quality of a thin-walled rectangular tube during the rotary draw bending process.

Keywords Thin-walled rectangular tube · Rotary draw bending · Collapsing deformation · Analytical model

1 Introduction

The numerical control (NC) rotary draw bending technology of a thin-walled rectangular tube has attracted more and more applications in various high-technology industries, such as aviation, aerospace, radar, and satellite communications, due to its realization of the manufacturing of a thin-walled bent rectangular tube accurately, flexibly, and efficiently [1]. However, the bending is a complex process with multi-nonlinearity under multi-dies constraints, and the cross-section distortion is the key factor determining the bending limit and quality during the process with small bending radius. The cross-section distortion is mainly induced by the collapsing deformation of the outer flange during the bending process. The analytical solution can provide designers a more global view in terms of the general tendency and the effect of individual parameters on the forming quality of the rectangular tube. Therefore, it is necessary to establish an analytical model to describe the collapsing deformation of a thin-walled rectangular tube during the rotary draw bending process.

Great efforts have been made previously for cross-section distortion in bending processes of tubes with different sections. The collapsing deformation of thin-walled box section beams in pure bending process was studied through combined experiment and analytical analysis by Kecman [2], and mathematical equations were developed to predict the axial and bending resistance based on limit analysis. Cimpoeru [3] investigated the large deflection of a thin-walled square tube experimentally and obtained the relationship between the bending moment and angle of rotation. It was found that a small tension could affect the post suck-in deformation greatly. Kim [4] studied the bending collapse of thin-walled rectangular columns and established a new collapse mechanism analytically. Stretch bending of a rectangular tube was investigated by Clausen [5, 6] experimentally and numerically, and a numerical model using the code LS-DYNA was obtained. An efficient formulation was presented by Corona [7] to predict the cross-section distortion and springback of extrusions with arbitrary, thin-walled cross section, and it was found that higher tensions induced a relatively large, permanent cross-section distortion. In reference [8], the authors investigated the shearing bending process of a circular tube experimentally, and an elastoplastic 3D finite element simulation was conducted, aimed at clarifying the forming mechanism. Miller [9–11] made a systematic study on the effects of tension and pressure on distortion and then established 2D and 3D analytical models of the bend–stretch forming. The

K. X. Liu · Y. L. Liu (✉) · H. Yang
State Key Laboratory of Solidification Processing,
School of Materials Science and Engineering,
Northwestern Polytechnical University, P.O. Box 542,
Xi'an 710072, People's Republic of China
e-mail: lyl@nwpu.edu.cn

analytical expressions were derived by Zhu [12, 13] for the amount of distortion and the needed internal pressure in stretch bending of the rectangular tube based on energy minimization. The analytical models were developed by Paulsen [14–16] to predict the distortion of cross-section members in the stretch bending of a rectangular tube based on the plastic theory and the energy method. Most of these studies are focused on stretch bending and pure bending, and the effects of dies are neglected. Although they have played positive roles on studies of tube bending, all the investigations are confined to pure bending instead of considering the potential effects of bending modes and other externally applied forces. A comprehensive computer-based methodology, Tube ProDes, is proposed for process design of the rotary draw bending of tubes [17]. It is useful for us to design and manufacture various dies in rotary draw bending of tubes. In reference [18], the effect of the internal pressure on the cross-section ovality, wall thickness, and wall thickening was studied for the rotary draw bending of aluminum alloy tubes. For the rotary draw bending process of a thin-walled rectangular tube, it is a complex forming process under the coordination of multi-dies, and the effects of dies on forming quality of rectangular tube are significant. These studies are mainly carried out by finite element (FE) simulation [19, 20]. Up to now, the analytical analysis on the effects of various dies on collapsing deformation for the rectangular tube during the rotary draw bending process is scarcely reported previously.

In this paper, the effects between rectangular tube and dies are analyzed, and the force between the outer flange and core and the bending moment acted by the clamp die are obtained analytically. Under these loads, the collapsing deformation function of the outer flange is deduced based on the small deflection hypothesis and the theory of plate and shell. And then, the analytical model is validated by comparison with experimental and FE-simulated results.

2 The establishment of analytical model for collapsing deformation of outer flange

2.1 The simplified model for loads and deformation of outer flange

The rotary draw bending of a thin-walled rectangular tube is shown in Fig. 1. In the bending process, the forward parts of the tube are clamped by the clamp die and clamp insert die externally and supported by a clamp plug die internally. The clamp die provides a bending moment to force the tube to bend around the bending die. The backward parts are clamped by a pressure die and wiper die externally and supported by a mandrel die internally. The pressure die gives a boost force at a certain boost velocity. It can be considered that the forward and backward zones of the bent tube are clamped tightly by the dies against the deformation. The mandrel and cores are inserted into the hollow tube to prevent cross-section distortion. Therefore, there are only two dies affecting the deformation of the outer flange directly, i.e., clamp die and core die. The collapsing deformation w (as shown in Fig. 1) can be divided into two parts: w_{qc} (as shown in Fig. 2a) acted by force q_c between cores and outer flange and w_M (as shown in Fig. 2b) acted by bending moment M provided by the clamp die. Because both deformations are in opposite directions, the total collapsing deformation w is given in Eq. (1).

$$w = w_M - w_{qc} \tag{1}$$

2.2 The analytical analysis of force q_c acted by cores and bending moment M acted by clamp die

In the bending process, the rectangular tube is cut away along the bending direction and width direction, as shown in Fig. 3. To analyze the stress of the tube, the element is extracted from the outer flange. The stress acted on the

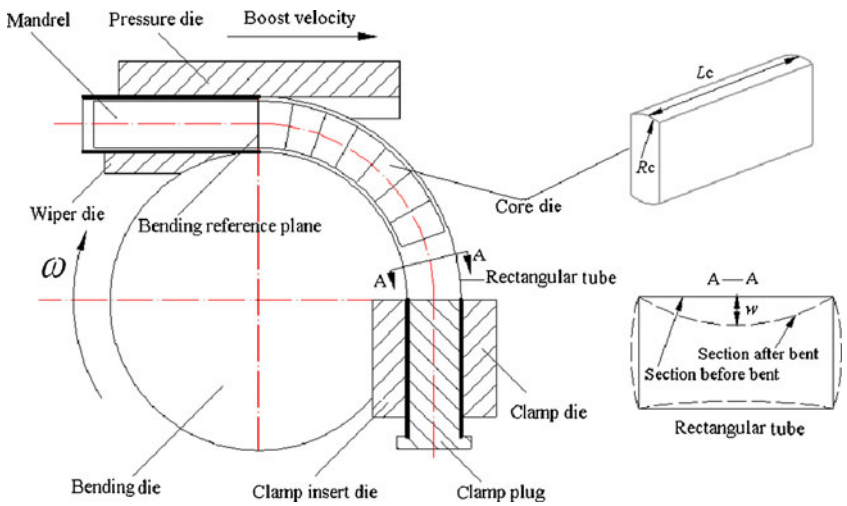

Fig. 1 Schematic diagram of NC tube bending

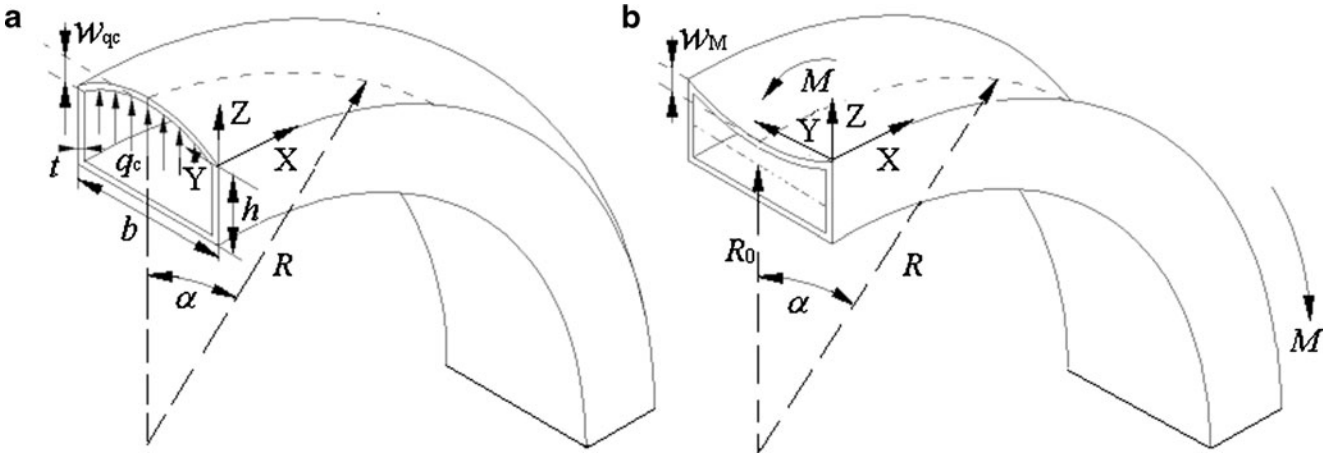

Fig. 2 The collapsing deformation of outer flange: (**a**) w_{qc} acted by force q_c, (**b**) w_M acted by bending moment M

element is shown in Fig. 4, including σ_α in the bending direction, σ_β in the width section, and σ_γ in the radial direction. The stress equilibrium equations of the element are given in Eq. (2) in the width direction and Eq. (3) in the bending direction.

$$\begin{aligned}&[(\sigma_r+d\sigma_r)(r+dr)d\beta(R+dR)d\alpha-\sigma_r rRd\beta d\alpha]\quad\cos\beta\\&-\left[(\sigma_\beta+d\sigma_\beta)dr(R+dR)d\alpha-\sigma_\beta Rdrd\alpha\right]\sin\beta+\sigma_\alpha rdrd\alpha d\beta=0\end{aligned}\tag{2}$$

$$\begin{aligned}&[(\sigma_r+d\sigma_r)(r+dr)d\beta(R+dR)d\alpha-\sigma_r rRd\beta d\alpha]\sin\beta\\&+\left[(\sigma_\beta+d\sigma_\beta)dr(R+dR)d\alpha-\sigma_\beta Rdrd\alpha\right]\cos\beta=0\end{aligned}\tag{3}$$

where α is the angle between the section and bending reference plane; β is the angle between the section and the middle section; r and R are the bending radius of the outer flange in the width direction and bending direction, respectively; R_0 is the bending radius of the rectangular tube, as shown in Fig. 2b. In the bending process, the geometric relationship between R_0 and R is given in Eq. (4).

$$R\approx R_0+h\Big/2\tag{4}$$

where h is the height of the rectangular tube.

By (3)×cos β−(2)×sin β and then eliminating $drd\alpha$ in both sides, Eq. (5) can be given:

$$Rd\sigma_\beta+\sigma_\beta dR=\sigma_\alpha r\sin\beta d\beta\tag{5}$$

It can be converted into Eq. (6):

$$d\left(R\sigma_\beta\right)=\sigma_\alpha r\sin\beta d\beta\tag{6}$$

In the bending process, the variation of flange width can be neglected. So the following equation can be derived as

$$r\sin\beta d\beta=dl_\beta\tag{7}$$

where l_β is the arc length corresponding to the angle β in the width direction.

Substituting Eq. (7) into Eq. (6), Eq. (6) can be written as

$$d\left(R\sigma_\beta\right)=\sigma_\alpha dl_\beta\tag{8}$$

It is mentioned that the circumferential stress is 0 in the middle section according to the symmetrical character. The boundary condition can be written as β=0, l_β=0, σ_β=0. Integrating Eq. (8) and combining the boundary condition, Eq. (9) can be derived as

$$R\sigma_\beta=\sigma_\alpha l_\beta\tag{9}$$

For the rectangular tube with dimensions 24.86×12.2×1 mm, the width/thickness ratio is up to 24.86, and it is bigger than 15. Therefore, the outer flange is seen as a shell in the analytical model. So the radial stress is neglected.

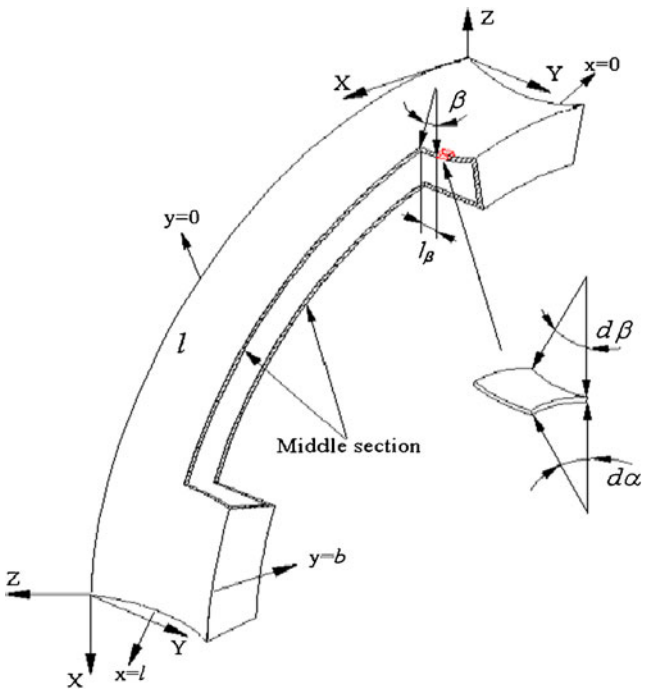

Fig. 3 The cutaway in three views and the element extracted from the outer flange

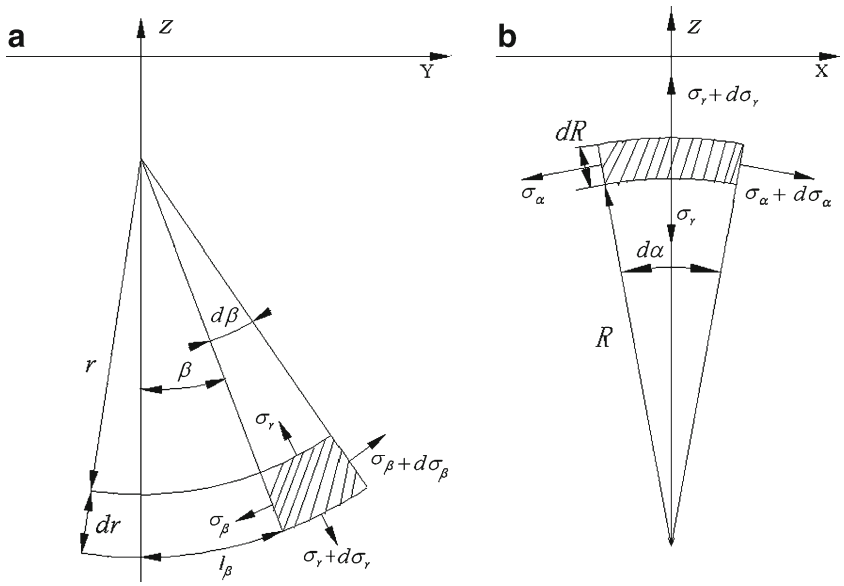

Fig. 4 The stress of element shown in two views: **a** in the width direction, **b** in the bending direction

According to the Tresca yield criterion, the relationship between σ_α and σ_β is given as

$$\sigma_\alpha - \sigma_\beta = \sigma_s \tag{10}$$

where σ_s is the yield strength of the tube material.

By the combination of Eqs. (9) and (10), the following expression can be given as

$$\sigma_\alpha = \frac{R_0 + {}^{h}/_{2}}{R_0 + {}^{h}/_{2} - l_\beta}\sigma_s, \quad \sigma_\beta = \frac{l_\beta}{R_0 + {}^{h}/_{2} - l_\beta}\sigma_s \tag{11}$$

In the bending process, the tube and core die are compressed to contact in the local area. The relationship between the contacted stress and the external force is highly nonlinear, so it is difficult to obtain q_c between the core die and rectangular tube from the external force acting on the tube. The Hertz theory is initially restricted to frictionless surface and perfectly elastic solids. However, the development of the theories of plasticity and linear viscoelasticity has enabled the stresses and deformations at the contact of inelastic bodies to be examined [21, 22]. The large lubricant is applied in the core–tube interface to reduce the friction between core die and tube. The core die is simplified as rigid with no deformation, and plastic deformation of the rectangular tube had occurred in the bending process. Therefore, it is reasonable to obtain the stress between tube and core die q_c according to the Hertz contact theory. The core and outer flange can be seen as cylinders. Initially, the flange and core are contacted at one point and then in a surface. So the force q_c between cores and outer flange can be obtained as follows:

$$q_c = \frac{2\pi L_c^2 \sigma_\alpha^2 C^2 R_c R\left(\frac{1-\mu_c^2}{E_c} + \frac{1-\mu^2}{E}\right)}{(R-R_c)\left(C^2 + l^2\right)} \tag{12}$$

where μ and μ_c is the Poisson ratio of tube and cores, respectively; C is the clearance between core and outer flange; l, as shown in Fig. 3, is the arc length of the flange in the bending zone; l_c is the length of the core; R_c is the radius of the core, as shown in Fig. 1; and E_c and E are Young's modulus of the cores and tube, respectively.

Assuming the core is seen as a rigid body, i.e., $E_c \to +\infty_c$, and $C \ll l$, Eq. (12) can be simplified to:

$$q_c = \frac{2\pi L_c^2 \sigma_\alpha^2 C^2 R_c R(1-\mu^2)}{E(R-R_c)l^2} \tag{13}$$

According to the principle of virtual work, the total bending moment that acted on the outer flange can be determined as

$$M = 2\int_0^{b/2} \frac{\sigma_\alpha t h}{2} dl_\beta = th\left(R_0 + h/2\right)\ln\left(\frac{R_0 + h/2}{R_0 + h/2 - b/2}\right)\sigma_s \tag{14}$$

where t and b are the thickness and width of the rectangular tube, respectively.

2.3 The determination of collapsing deformation

2.3.1 The equilibrium function of outer flange

For a plate subjected to the force, the following differential equation should be satisfied according to the theory of plate and shell.

$$\frac{\partial^4 w}{\partial x^4} + 2\frac{\partial^4 w}{\partial x^2 \partial y^2} + \frac{\partial^4 w}{\partial y^4} = \frac{q}{D} \tag{15}$$

where w is the collapsing deformation of the outer flange, $D = \frac{Et^3}{12(1-\mu^2)}$ is the flexural rigidity of the outer flange, and q is the transverse load on the outer flange.

To determine the collapsing deformation function, firstly, the general solution is obtained through solving the differential equation. And then, the coefficients of the general solution are derived by combination with the boundary conditions. The collapsing deformation function is obtained finally.

2.3.2 The collapsing deformation w_{qc} acted by force q_c between cores and outer flange

The collapsing deformation w_{qc} is disintegrated into two parts according to single trigonometric series as shown in Eq. (16).

$$w_{qc} = \sum_m f_m(x)\sin\frac{m\pi y}{b} \tag{16}$$

The force q_c between core and outer flange is also expanded in single trigonometric series as follows:

$$q_c = \sum_m q_m(x)\sin\frac{m\pi y}{b} \tag{17}$$

So it can be obtained that

$$q_m(x) = \frac{2}{b}\int_0^b q_c\sin\frac{m\pi y}{b}dy = \frac{2q_c}{m\pi}(1-\cos m\pi) \tag{18}$$

And it can be simplified as:

$$q_m(x) = \begin{cases} \dfrac{4q_c}{m\pi}\,(m = 1,3,5,\cdots) \\ 0\ (m = 2,4,6,\cdots) \end{cases} \tag{19}$$

Substituting Eqs. (16) and (18) into the differential Eq. (15), it can be derived

$$f_m''''(x) - 2\left(\frac{m\pi}{b}\right)^2 f_m''(x) + \left(\frac{m\pi}{b}\right)^4 f_m(x) = \frac{q_m(x)}{D} \tag{20}$$

It is employed that

$$f^* = \frac{2q_c b^4}{D\pi^5 m^5}(1-\cos m\pi) \tag{21}$$

It is easy to confirm that f^* is the particular solution of Eq. (20). And the general solution of Eq. (20) can be given as follows:

$$f_m(x) = A_m\mathrm{ch}\frac{m\pi x}{b} + B_m\mathrm{sh}\frac{m\pi x}{b} + C_m\frac{m\pi x}{b}\mathrm{ch}\frac{m\pi x}{b} + D_m\frac{m\pi x}{b}\mathrm{sh}\frac{m\pi x}{b} \tag{22}$$

So the solution of Eq. (20) is calculated as:

$$f_m(x) = A_m\mathrm{ch}\frac{m\pi x}{b} + B_m\mathrm{sh}\frac{m\pi x}{b} + C_m\frac{m\pi x}{b}\mathrm{ch}\frac{m\pi x}{b} + D_m\frac{m\pi x}{b}\mathrm{sh}\frac{m\pi x}{b} + f^* \tag{23}$$

For the collapsing deformation w_{qc} acted by force q_c between core and tube, the boundary condition can be supposed that two edges of the outer flange in the bending direction are simply supported, and the other two edges of the outer flange in the width direction are fully fixed. Therefore, the boundary conditions can be given by combination Fig. 2a with Fig. 3.when

$$x = 0, l, w_{qc} = 0, \frac{\partial w_{qc}}{\partial y} = 0;\ \ y = 0, b,\ \ w_{qc} = 0 \tag{24}$$

where $x=R\alpha$, α the angle between the section and bending reference plane.

Substituting Eq. (24) into Eq. (23), the coefficients in Eq. (23) are given as

$$A_m = -f^*,\ \ B_m = \frac{\mathrm{ch}k_m - 1}{\mathrm{sh}k_m + k_m}f^*,\ \ C_m = -\frac{\mathrm{ch}k_m - 1}{\mathrm{sh}k_m + k_m}f^*,\ \ D_m = \frac{\mathrm{sh}k_m}{\mathrm{sh}k_m + k_m}f^* \tag{25}$$

where $k_m = \frac{m\pi b}{l}$

So the collapsing deformation function acted by the force between core and outer flange is obtained:

$$w_{qc} = \sum_{m=1}^{\infty}\left(\begin{array}{l} -\mathrm{ch}\dfrac{m\pi x}{b} + \dfrac{\mathrm{ch}k_m - 1}{\mathrm{sh}k_m + k_m}\mathrm{sh}\dfrac{m\pi x}{b} - \dfrac{\mathrm{ch}k_m - 1}{\mathrm{sh}k_m + k_m}\dfrac{m\pi x}{b}\mathrm{ch}\dfrac{m\pi x}{b} \\ + \dfrac{\mathrm{sh}k_m}{\mathrm{sh}k_m + k_m}\dfrac{m\pi x}{b}\mathrm{sh}\dfrac{m\pi x}{b} + 1 \end{array}\right) f^*\sin\frac{m\pi y}{b} \tag{26}$$

2.3.3 The collapsing deformation w_M acted by bending moment M

For the collapsing deformation w_M acted by bending moment M, there is no transverse load acted on the flange, so q_M=0. And then function (15) can be simplified as

$$\nabla^2\nabla^2 w_M = 0 \tag{27}$$

It is easy to determine that w_M=0 is the particular solution of Eq. (27). And the general solution is given as

$$w_M(x,y) = \sum_{n=1}^{\infty}\left(a_n\mathrm{ch}\frac{n\pi x}{b} + b_n\mathrm{sh}\frac{n\pi x}{b} + c_n\frac{n\pi x}{b}\mathrm{ch}\frac{n\pi x}{b} + d_n\frac{n\pi x}{b}\mathrm{sh}\frac{n\pi x}{b}\right)\sin\frac{n\pi y}{b} \tag{28}$$

For the collapsing deformation w_M acted by bending moment M provided by the clamp die, the boundary condition can be supposed that four edges of the outer flange are simply supported. The boundary conditions can be given in the following equation by the combination of Fig. 2b with Fig. 3.

when

$$x=0,l,w_M=0,D\frac{\partial^2 w_M}{\partial x^2}=M;\text{when } y=0,b,w_M=0 \tag{29}$$

Substituting Eq. (29) into Eq. (28), the coefficients are given as

$$a_n=0,b_n=\frac{\mathrm{sh}\frac{n\pi l}{b}+3\mathrm{ch}\frac{n\pi l}{b}-3}{\mathrm{sh}\frac{n\pi l}{b}}\left(\frac{b}{m\pi}\right)^3 M,$$

$$c_n=\frac{1-\mathrm{ch}\frac{n\pi l}{b}}{\mathrm{sh}\frac{n\pi l}{b}}\left(\frac{b}{m\pi}\right)^3 M,d_n=\frac{\mathrm{ch}\frac{n\pi l}{b}-1}{\frac{n\pi l}{b}-\mathrm{sh}\frac{n\pi l}{b}}\left(\frac{b}{m\pi}\right)^3 M \tag{30}$$

So the collapsing deformation w_M acted by bending moment M can be derived as

$$w_M(x,y)=\sum_{n=1}^{\infty}\left(\begin{array}{l}\frac{\mathrm{sh}\frac{n\pi l}{b}+3\mathrm{ch}\frac{n\pi l}{b}-3}{\mathrm{sh}\frac{n\pi l}{b}}\mathrm{sh}\frac{n\pi x}{b}\\ +\frac{1-\mathrm{ch}\frac{n\pi l}{b}}{\mathrm{sh}\frac{n\pi l}{b}}\frac{n\pi x}{b}\mathrm{ch}\frac{n\pi x}{b}+\frac{\mathrm{ch}\frac{n\pi l}{b}-1}{\frac{n\pi l}{b}-\mathrm{sh}\frac{n\pi l}{b}}\frac{n\pi x}{b}\mathrm{sh}\frac{n\pi x}{b}\end{array}\right)\left(\frac{b}{n\pi}\right)^3 M\sin\frac{n\pi y}{b} \tag{31}$$

Finally, substituting Eqs. (26) and (31) into Eq. (1), the total collapsing deformation of outer flange w can be obtained analytically.

$$\begin{aligned}w_M=&\sum_{n=1}^{\infty}\left(\begin{array}{l}\frac{\mathrm{sh}\frac{n\pi l}{b}+3\mathrm{ch}\frac{n\pi l}{b}-3}{\mathrm{sh}\frac{n\pi l}{b}}\mathrm{sh}\frac{n\pi x}{b}\\ +\frac{1-\mathrm{ch}\frac{n\pi l}{b}}{\mathrm{sh}\frac{n\pi l}{b}}\frac{n\pi x}{b}\mathrm{ch}\frac{n\pi x}{b}+\frac{\mathrm{ch}\frac{n\pi l}{b}-1}{\frac{n\pi l}{b}-\mathrm{sh}\frac{n\pi l}{b}}\frac{n\pi x}{b}\mathrm{sh}\frac{n\pi x}{b}\end{array}\right)\left(\frac{b}{n\pi}\right)^3 M\sin\frac{n\pi y}{b}\\ &-\sum_{m=1}^{\infty}\left(\begin{array}{l}-\mathrm{ch}\frac{m\pi x}{b}+\frac{\mathrm{ch}k_m-1}{\mathrm{sh}k_m+k_m}\mathrm{sh}\frac{m\pi x}{b}-\frac{\mathrm{ch}k_m-1}{\mathrm{sh}k_m+k_m}\frac{m\pi x}{b}\mathrm{ch}\frac{m\pi x}{b}\\ +\frac{\mathrm{sh}k_m}{\mathrm{sh}k_m+k_m}\frac{m\pi x}{b}\mathrm{sh}\frac{m\pi x}{b}+1\end{array}\right)f^*\ \sin\frac{m\pi y}{b}\end{aligned} \tag{32}$$

The collapsing deformation w for 3A21 aluminum alloy thin-walled rectangular tube when m, n=1, m, n=3, and m, n=5 are listed in Table 1, respectively. It can be seen that the collapsing deformation when m, n=3, and m, n=5 is infinitesimal to the collapsing deformation when m, n=1. So the simplest case of m, n=1 is selected to measure the collapsing deformation of the outer flange within the acceptable accuracy, and Eq. (32) is simplified as shown in Eq. (33).

$$\begin{aligned}w=&\left(\begin{array}{l}\frac{\mathrm{sh}k+3\mathrm{ch}k-3}{\mathrm{sh}k}\mathrm{sh}\frac{\pi x}{b}\\ +\frac{1-\mathrm{ch}k}{\mathrm{sh}k}\frac{\pi x}{b}\mathrm{ch}\frac{\pi x}{b}+\frac{\mathrm{ch}k-1}{k-\mathrm{sh}k}\frac{\pi x}{b}\mathrm{sh}\frac{\pi x}{b}\end{array}\right)\quad\left(\frac{b}{\pi}\right)^3 M\sin\frac{\pi y}{b}\\ &-\left(-\mathrm{ch}\frac{\pi x}{b}+\frac{\mathrm{ch}k-1}{\mathrm{sh}k+k}\mathrm{sh}\frac{\pi x}{b}-\frac{\mathrm{ch}k-1}{\mathrm{sh}k+k}\frac{\pi x}{b}\mathrm{ch}\frac{\pi x}{b}+\frac{\mathrm{sh}k}{\mathrm{sh}k+k}\frac{\pi x}{b}\mathrm{sh}\frac{\pi x}{b}+1\right)f^*\sin\frac{\pi y}{b}\end{aligned} \tag{33}$$

Table 1 The value of collapsing deformation w

The angle (°)	m, n=1	m, n=3	m, n=5
0	0.2311	0	0
2.25	0.28856	0.000687	0.000115
4.5	0.30811	0.001043	4.91E−05
6.75	0.34679	0.003125	0.000178
9	0.39181	0.003742	0.000259
11.25	0.43783	0.001345	4.26E−05
13.5	0.4826	0.000826	0.000192
15.75	0.52635	0.006483	0.000836
18	0.56874	0.001741	0.000217
20.25	0.60888	0.002218	0.00013
22.5	0.64647	0.005455	0.000239
24.75	0.68053	0.006839	0.000549
27	0.711	0.001927	2.1E−05
29.25	0.73833	0.000781	0.000281
31.5	0.76101	0.009307	0.001183
33.75	0.77995	0.002926	0.00027
36	0.79558	0.00306	0.000206
38.25	0.80668	0.006321	0.000186
40.5	0.81516	0.008565	0.000774
42.75	0.82047	0.001887	3.38E−05
45	0.82199	0.000351	0.000288
47.25	0.82033	0.009914	0.001231
49.5	0.81565	0.003624	0.000239
51.75	0.80724	0.003223	0.000236
54	0.79608	0.005736	8.03E−05
56.25	0.78087	0.008527	0.000847
58.5	0.76172	0.001405	8.55E−05
60.75	0.73885	0.000131	0.000226
63	0.71192	0.008461	0.001014
65.25	0.68145	0.003497	0.000151
67.5	0.64727	0.002643	0.000202
69.75	0.60975	0.003997	1.09E−05
72	0.56959	0.006428	0.000689
74.25	0.52706	0.00071	9.54E−05
76.5	0.4835	0.000364	0.000121
78.75	0.43867	0.005101	0.000584
81	0.39208	0.00228	5.23E−05
83.25	0.34683	0.001427	0.000111
85.5	0.30827	0.001814	3.8E−05
87.75	0.28789	0.003339	0.00038
90	0.23024	0.000187	5.63E−05

3 Validation of the analytical model

3.1 The comparison between the analytical and experimental collapsing deformation

The geometric dimensions of rectangular tube and cores used are shown in Table 2. The material of the rectangular tube is 3A21 aluminum alloy, and the material parameters are obtained by tensile test using CSS-44100 electric universal testing machine, shown in Table 3. The analytical and experimental studies are conducted respectively in the conditions as shown in Table 4.

Table 2 The geometric dimensions of core and 3A21 aluminum alloy rectangular tube

Experimental parameters	The value
Core length L_c/mm	22.66
Radius of cores R_c/mm	5
The height of rectangular tube h/mm	12.2
The width of rectangular tube b/mm	24.86
The thickness of rectangular tube t/mm	1

The experiments are conducted in the NC bending machine W27YPC-63, as shown in Fig. 5a. And all the various dies used are shown in Fig. 5b. The tube after being bent is shown in Fig. 6. To investigate the collapsing deformation of the outer flange during the rotary draw bending process of the rectangular tube, the sections are selected in the bent zone of the tube shown in Fig. 7, and the angle between the two adjacent sections is 10°. The section of angle 0° is the bending reference plane unchanged with the bending process. The collapsing deformation obtained by experiment is shown in Fig. 8.

In order to predict the collapsing deformation thoroughly and precisely, the sections are selected in the bent zone of the tube, and the angle between the two adjacent sections is 2.25°. Substituting the data in Tables 2, 3, and 4 into Eq. (1), the collapsing deformation of the outer flange using the analytical model can be obtained, and then the result is shown in Fig. 8.

From Fig. 8, it can be observed that the collapsing deformation of the outer flange increases firstly and then decreases with the bending angle. And the maximum collapsing deformation is located in the cross section with angles of 40–50°, which is in the same tendency as that of the experimental result. The error between analytical and experimental collapsing deformation does not exceed 15 %. Good agreement between analytical and experimental collapsing deformation is found. So it can be concluded that the proposed analytical model of collapsing deformation is validated to be credible.

Table 3 The material parameters of 3A21 aluminum alloy

Experimental parameters	The value
Elastic modulus E/GPa	60.2
Yield strength σ_s/MPa	120
Poisson's ratio μ	0.33

Table 4 The process parameters used in experiment, analytical analysis, and FE simulation

Parameters	Experimental value	Analytical value	Simulated value
Bending angle θ/°	90	90	90
Bending radius R/mm	40	40	40
Core number n	3	Tube is supported fully in bent zone	3
Friction state between mandrel and tube	Lubricated by aero oil	–	0.1
Friction state between clamp dies and tube	Dry friction	–	0.7
Clearances between dies and tube/mm	0.1	0.1	0.1

3.2 The comparison between the analytical and FE-simulated collapsing deformation

A 3D FEM model of rotary draw bending of a thin-walled rectangular tube is built under the ABAQUS/Explicit environment as shown in Fig. 9. The model has been validated to be credible[19]. The rectangular tube is meshed using linear, four-node shell elements with reduced integration (S4R). Four-node 3D bilinear rigid quadrilateral discrete rigid elements are selected to describe the discrete rigid dies during the bending process. The collapsing deformation of the outer flange is obtained by using process parameters listed in Table 3, and then it is also shown in Fig. 8.

It can be seen that the collapsing deformation of the outer flange obtained from FE simulation and analytical analysis is symmetrical with the section of 45° from Fig. 8. The difference between analytical and FE-simulated collapsing deformation in the middle zone is minor, and the difference

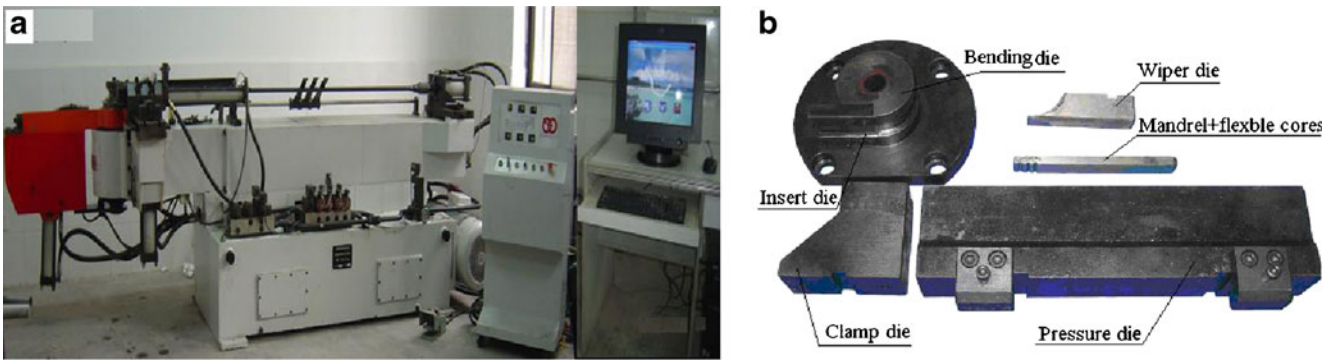

Fig. 5 Tube bender and dies: **a** NC bending machine W27YPC-63, **b** various dies

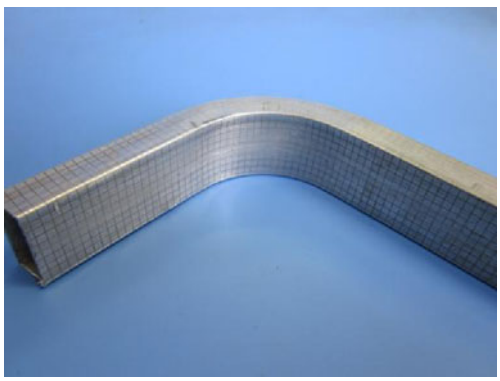

Fig. 6 The tube after being bent by experiment

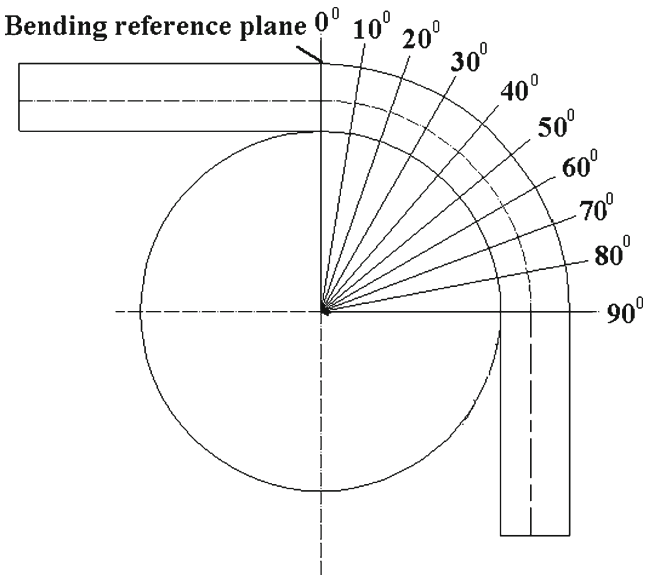

Fig. 7 Sections selected in the bent zone of the tube

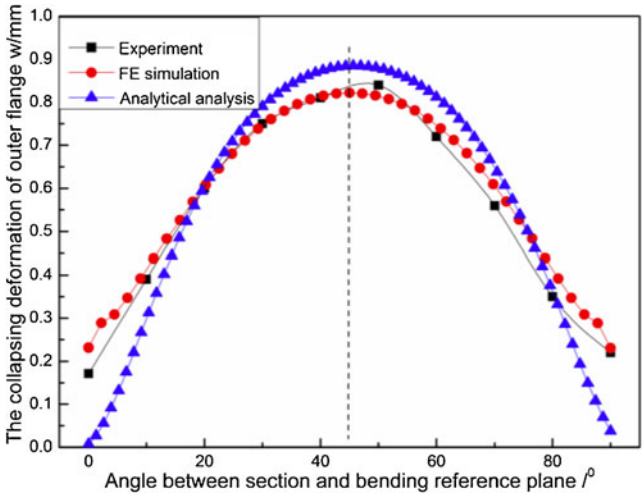

Fig. 8 The comparison among analytical, simulated, and experimental collapsing deformation

in the forward and backward zone is major. Fortunately, the major difference is within acceptable limits of 20 %.

In the backward zone between the sections with the angle of 0° and 20° and the forward zone between the sections with the angle of 70° and 90°, the collapsing deformation obtained by the analytical model is the smallest. The reason is that in the analytical model, it is supposed that the tube cannot deform in the two terminals under the constraint of dies. However, the tube can deform in a small scale by experiment and FE simulation. In the zone between the sections with the angle of 20° and 70°, the collapsing deformation obtained by analytical model is the biggest. In order to elevate the computational efficiency, the single trigonometric series of collapsing deformation is simplified with $n=1$. It induces that the collapsing deformation obtained by the analytical analysis is bigger than those obtained by FE simulation and experiment.

In addition, the analytical approach has a great advantage over FE simulation and experiment in computational time and convenience. It would take much work and time to assembly the dies experimentally, and a trial-and-error approach costs highly. Even though the mass scaling factor of 10,000 is adopted to reduce the computation time for FE simulation, it still takes 25 h of CPU time to simulate the collapsing deformation. By using the presented analytical model, usually less than 100 s is needed. From this point of view, the analytical method provides an efficient way of predicting the collapsing deformation of the outer flange.

4 Conclusions

1. The constraints of various dies on the rectangular tube in the rotary draw bending process are analyzed, and the simplified model for loads and deformation of outer flange is made. Based on the simplified model, the force between core and outer flange is obtained according to Hertz contact theory, and the bending moment acted by the clamp die is derived by principle of virtual work.
2. The collapsing deformation function of the outer flange is divided into two parts: one acted by force between core and outer flange, and the other acted by bending moment. Based on the small deflection hypothesis and theory of plate and shell, the analytical model for the collapsing deformation is established employing the single trigonometric series.
3. The analytical, experimental, and FE-simulated collapsing deformation of the thin-walled rectangular tube in rotary draw bending processes are investigated respectively. It is found that the collapsing deformation of the outer flange obtained by analytical model agrees well with the results obtained by experiment and FE simulation. It is validated that the analytical model for the collapsing deformation of the thin-walled rectangular tube in rotary draw bending process is credible and efficient.

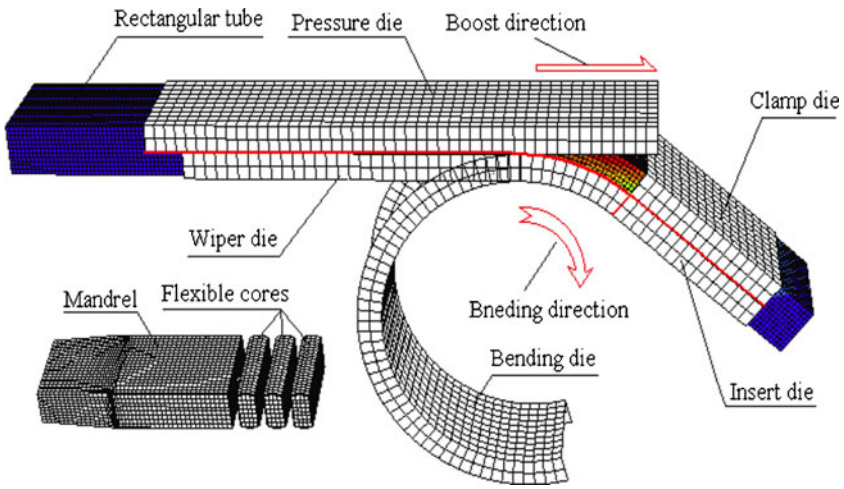

Fig. 9 3D FE simulation model using ABAQUS

Acknowledgments The authors would like to thank the National Natural Science Foundation of China (no. 50975235 and 50575184) and 111 Project (no. B08040) for the support given to the research.

References

1. Yang H, Zhan M, Liu YL (2004) Some advanced plastic processing technologies and their numerical simulation. J Mater Process Tech 151:63–69
2. Kecman D (1983) Bending collapse of rectangular and square section tubes. Int J Mech Sci 25:623–636
3. Cimpoeru SJ, Murray NW (1993) The large-deflection pure bending properties of a square thin-walled tube. Int J Mech Sci 35(3–4):247–256
4. Kim TH, Reid SR (2001) Bending collapse of thin-walled rectangular section columns. Comput Struct 79:1897–1911
5. Clausen AH, Hopperstad OS, Langseth M (2000) Stretch bending of aluminium extrusions for car bumpers. J Mater Process Tech 102:241–248
6. Clausen AH, Hopperstad OS, Langseth M (2001) Sensitivity of model parameters in stretch bending of aluminium extrusions. Int J Mech Sci 43:427–453
7. Corona E (2004) A simple analysis for bend-stretch forming of aluminum extrusions. Int J Mech Sci 46:433–448
8. Goodarzi M, Kuboki T, Murata M (2007) Effect of die corner radius on the formability and dimensional accuracy of tube shear bending. Int J Adv Manuf Technol 35:66–74
9. Miller JE, Kyriakides S, Bastard AH (2001) On bend-stretch forming of aluminum extruded tubes-I: experiments. Int J Mech Sci 43:1283–1317
10. Miller JE, Kyriakides S, Corona E (2001) On bend-stretch forming of aluminum extruded tubes-II: analysis. Int J Mech Sci 43:1319–1338
11. Miller JE, Kyriakides S (2003) Three dimensional effects of the bend stretch forming of aluminum tubes. Int J Mech Sci 45(1):115–140
12. Zhu H, Stelson KA (2002) Distortion of rectangular tubes in stretch bending. J Manuf Sci E-T ASME 124(4):886–890
13. Zhu H, Stelson KA (2003) Modeling and closed-loop control of stretch bending of aluminum rectangular tubes. J Manuf Sci E-T ASME 125:113–119
14. Paulsen F, Welo T (2001) Cross-sectional deformations of rectangular hollow sections in bending: part I—experiments. Int J Mech Sci 43:109–129
15. Paulsen F, Welo T (2001) Cross-sectional deformations of rectangular hollow sections in bending: part II—analytical models. Int J Mech Sci 43:131–152
16. Paulsen F, Welo T, Sovik OP (2002) A design method for prediction of dimensions of rectangular hollow sections formed in stretch bending. J Mater Process Tech 128:48–66
17. Strano M (2005) Automatic tooling design for rotary draw bending of tubes. Int J Adv Manuf Technol 26:733–740
18. Lazarescu L (2013) Effect of internal fluid pressure on quality of aluminum alloy tube in rotary draw bending. Int J Adv Manuf Technol 64:85–91
19. Zhao GY, Liu YL, Yang H, Lu CH, Gu RJ (2009) Three-dimensional finite-elements modeling and simulation of rotary-draw bending process for thin-walled rectangular tube. Mater Sci Eng, A 499:257–261
20. Zhao GY, Liu YL, Yang H (2010) Effect of clearance on wrinkling of thin-walled rectangular tube in rotary-draw bending process. Int J Adv Manuf Tech 50(1–4):85–92
21. Johnson KL (2003) Contact mechanics [M]. Cambridge University Press, Cambridge, pp 84–104
22. Qian WC, Ye KY (1980) Elasticity mechanics [M]. Science Publishing House, Beijing, pp 312–327, in Chinese